Non-reflective Boundary Treatment for Fluid-Structure Interaction Simulation of Offshore Wind Turbine

Soo-Hong Jeon[1], *Jin-Rae Cho[2], Warn-Gyu Park[3]
and Weui-Bong Jeong[3]

[1], [2], [3] *School of Mechanical Engineering, Pusan National University, Busan 609-735, Korea*
[2] *jrcho@pusan.ac.kr* & *jrcho@midasit.com*

ABSTRACT

Fluid-structure interaction simulation of floating-type substructure of offshore wind turbine subject to under water explosion is addressed. The perfectly matched layer (PML) is used to suppress the wave reflection at the boundaries of finite flow domain which is truncated for the numerical simulation. The fluid-structure interaction induced by under water explosion is formulated by Eulerian non-viscous compressible Euler finite volume method and Lagrangian finite element method. It is confirmed through the numerical experiments that the PML successfully suppresses the wave reflection.

1. INTRODUCTION

The numerical analysis of structural dynamic response caused by the explosive wave under water is one of challenging subjects in fluid-structure interaction simulation. The structural dynamic responses of submarine and offshore substructure impacted by under water explosion become representative examples. The physical water domain of such phenomenon is infinite, but the consideration of the infinite water domain into the standard numerical methods is not possible. In most cases, the infinite domain is truncated based upon the analyst's own intuition and the appropriate boundary conditions are specified to the boundary of truncated finite simulation domain. However, one may experience the reflection of propagation wave from the boundary when the boundary condition option provided in the existing commercial hydro codes. Once the reflection phenomenon is not sufficiently suppressed the fluid-structure interaction simulation may, but frequently, lead to the time responses in big error. This paper addresses a non-reflective boundary treatment technique based upon the perfectly

---

[1] Graduate Student
[2] Vice Director
[3] Professor

matched layer (PML) (Berenger 1994; Hu 1996) for the fluid-structure interaction simulation of floating-type substructure subject to underwater explosion.

2. PROBLEM DESCRIPTION

The most important requirement of renewable energies is the efficiency and capacity, and in this regard wind power draws an intensive attention thanks to its potential to generate a huge amount of electricity from plenty of winds around us (Hansen and Hansen 2007). Wind turbines in the early stage were designed for the installation on the ground and showed the rapid increase in both the total installation number and the maximum power generation capacity. However, this worldwide trend encountered several obstacles such as the infringement of living environment and the limitation of being high-capacity and making large wind farm. This critical situation naturally turned the attention to the offshore sites, a less restrictive installation place.

2.1. Spar-type Floating Substructure of Offshore Wind Turbine

Offshore wind turbines are classified largely into two categories, fixed- and floating-type according to how the wind turbine tower is supported. Differing from the fixed-type, the floating-type wind turbine is under the concept design stage because several core technologies are not fully settled down (Karimirad et al. 2011). In particular, the design of floating substructure becomes a critical subject because it supports the entire wind turbine system and influences the dynamic stability. Currently, three types of floating substructures are considered, barge, tension leg (TLP) and spar types.
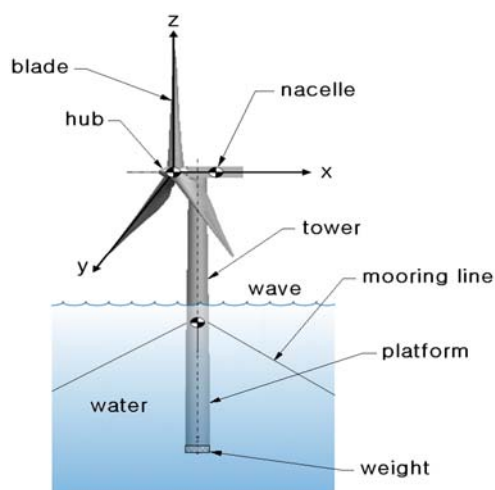

Fig. 1 Spar-type floating offshore wind turbine

A typical spar-type floating offshore wind turbine is represented in Fig. 1, where the entire wind turbine is supported by the buoyancy force and the vertical position is adjusted by the weight at the bottom of platform. The dynamic displacement of wind turbine which is caused by wind, wave and current loads is restricted by the tension of mooring lines (Lefebvre and Collu 2012). The dynamic stability of floating-type wind turbine is evaluated in terms of three translation (i.e., surge, sway and heave) and three rotation motions (i.e., pitch, roll and yaw) (Cho et al. 2012). These six degrees of

freedom are coupled to each other, and the pitch angle is the most significant parameter to evaluate the dynamic stability of wind turbine.

The dynamic stability of floating-type wind turbine is influenced by gust, wave and current, so most research efforts have been focused on the effects of such aero and hydro excitations. However, under water explosion gives rise to the fatal impact on the dynamic stability, even on the structural strength of wind turbine. Regarding the numerical simulation, the most critical problem is the truncation of semi-infinite flow domain to a finite one. This truncation of flow domain inherently may, but mostly, lead to the wave reflection at the boundaries, unless the special boundary treatment is devised. For the current study, the perfectly matched layer (PML) introduced by Berenger (1994) is extended to simulate the non-viscous compressible fluid-structure interaction induced by under water explosion.

2.2. Fluid-Structure Interaction Induced by Under Water Explosion

We denote $\Omega \in \Re^3$ be the deformed configuration of the floating platform, at the current time t, with the boundary $\partial\Omega = \overline{\partial\Omega_D \cup \partial\Omega_N}$. In which, $\partial\Omega_D$ indicates the essential boundary region and $\partial\Omega_N$ is the natural boundary region including the platform-wave interface $\partial\Omega_I$. The time-dependent displacement field $\boldsymbol{u}(\boldsymbol{x};t)$ of the floating platform is governed by

$$\sigma_{ij}(\boldsymbol{u})_{,j} + \rho(f_i - \ddot{u}_i) = 0, \quad in \quad \Omega \times (0,T] \tag{1}$$

with the initial conditions: $\boldsymbol{u}(\boldsymbol{x};0) = \boldsymbol{u}^0(\boldsymbol{x})$, $\dot{\boldsymbol{u}}(\boldsymbol{x};0) = \dot{\boldsymbol{u}}^0(\boldsymbol{x})$ and the boundary conditions: $\boldsymbol{u}(\boldsymbol{x};t) = \hat{\boldsymbol{u}}(\boldsymbol{x};t)$ on $\partial\Omega_D$ and $\sigma_{ij}(\boldsymbol{x};t)n_j = \hat{t}_i(\boldsymbol{x};t)$ on $\partial\Omega_N$. Where, σ_{ij} are Cauchy stresses, ρ and f are the density and the body force of platform, and $\hat{t}$ is the external traction including the hydrodynamic pressure p of water, respectively.

For the Eulerian formulation, the material domain $\Omega_F \in \Re^3$ of water is extended to a larger fixed domain such that it can fully cover the wave motion, where water and void regions are designated by $F_V = 1$ and $F_V = 0$ with the volume fraction $F_V \in [0,1]$ of water. By denoting $\widetilde{\Omega}_F \in \Re^3$ be the extended Eulerian domain, the non-viscous flow velocity V in the Eulerian kinematic description is governed by the mass conservation, the momentum equations and the energy equation given by

$$\frac{\partial \rho_F}{\partial t} + \nabla \cdot (\rho_F V) = 0, \quad in \quad \widetilde{\Omega}_F \times (0,T] \tag{2}$$

$$\frac{\partial (\rho_F V)}{\partial t} + (\rho_F V \cdot \nabla)V = \nabla \cdot \sigma^F, \quad in \quad \widetilde{\Omega}_F \times (0,T] \tag{3}$$

$$\frac{\partial (\rho_F e)}{\partial t} + \rho_F e \nabla \cdot V = -\nabla \cdot (pV), \quad in \quad \widetilde{\Omega}_F \times (0,T] \tag{4}$$

together with the volume fraction equation given by

$$\frac{\partial F_V}{\partial t} + V \cdot \nabla F = 0, \quad in \quad \widetilde{\Omega}_F \times (0,T] \tag{5}$$

with the initial conditions: $V(x;0) = 0$ and $F(x;0) = F_{ini}(x)$ and the boundary conditions: $V(x;t) \cdot n^F = \frac{\partial u}{\partial t} \cdot n^F$ on $\partial \Omega_I \times (0,T]$. Where, ρ_F is the water density, n^F the outward unit vector normal to the flow boundary, T the time period of observation, and e_3 the unit vector in the vertical direction. The total stress tensor of snow σ^F is defined by $\sigma^F = -p\mathbf{1}$ with $\mathbf{1}$ being the unit tensor.

The coupling between the displacement of platform and the wave is implemented by Euler-Lagrange coupling method, and the coupled fluid-structure interaction is solved by the staggered iterative scheme (Cho et al. 2006, 2008). The ignition and growth for both the un-reacted and the reaction products are calculated by he Jones-Wilkins-Lee (JWS) equation of state (EOS) (Lee and Tarver 1980) given by

$$p = A\left(1 - \frac{\omega\eta}{R_1}\right)e^{-R_1/\eta} + B\left(1 - \frac{\omega\eta}{R_2}\right)e^{-R_2/\eta} + \omega\eta\rho_0 e \tag{6}$$

with A, B, ω, R_1 and R_2 being the input constants of the un-reacted explosive.

3. PERFECTLY MATCHED LAYER

The extended Eulerian domain $\widetilde{\Omega}_F \in \Re^3$ is usually semi-infinite, so that its truncation is requisite for the numerical simulation. Let us denote $\hat{\Omega}_F \in \Re^3$ be the truncated simulation domain of $\widetilde{\Omega}_F$ and express the transport equations defined in Section 2 in the following generalized form,

$$\frac{\partial U}{\partial t} + \frac{\partial F}{\partial x} + \frac{\partial G}{\partial y} + \frac{\partial H}{\partial z} = 0, \quad in \quad \hat{\Omega}_F \times (0,T] \tag{7}$$

In which four vectors are defined by

$$U = \begin{Bmatrix} \rho_F \\ \rho_F V_x \\ \rho_F V_y \\ \rho_F V_z \\ \rho_F e \\ F_V \end{Bmatrix}, \quad F = \begin{Bmatrix} \rho_F V_x \\ \rho_F V_x^2 + p \\ \rho_F V_x V_y \\ \rho_F V_x V_z \\ (\rho_F e + p)V_x \\ F_V V_x \end{Bmatrix}, \quad G = \begin{Bmatrix} \rho_F V_y \\ \rho_F V_x V_y \\ \rho_F V_y^2 + p \\ \rho_F V_y V_z \\ (\rho_F e + p)V_y \\ F_V V_y \end{Bmatrix}, \quad H = \begin{Bmatrix} \rho_F V_z \\ \rho_F V_x V_z \\ \rho_F V_y V_z \\ \rho_F V_z^2 + p \\ (\rho_F e + p)V_z \\ F_V V_z \end{Bmatrix} \tag{8}$$

Referring to Fig. 2, the truncated simulation domain $\hat{\Omega}_F$ is decomposed of the interior domain and the PML domains. In the PML regions, U is divided into three and Eq. (7) is split into three equations given by

$$\frac{\partial U_1}{\partial t} + \frac{\partial F}{\partial x} + \sigma_x U_1 = 0 \tag{9}$$

$$\frac{\partial U_2}{\partial t} + \frac{\partial F}{\partial x} + \sigma_y U_2 = 0 \tag{10}$$

$$\frac{\partial U_3}{\partial t} + \frac{\partial F}{\partial x} + \sigma_z U_3 = 0 \tag{11}$$

In which, three parameters $(\sigma_x, \sigma_y, \sigma_z)$ called absorption coefficients introduced to absorb waves in the PML domains are greater than or equal to zero.

If three absorption coefficients are set by zero, then Eqs. (9)~(11) are reduced to the standard non-viscous Euler equations (2)~(5) defined in the extended Eulerian domain $\widetilde{\Omega}$ with $U = U_1 + U_2 + U_3$. Here, the condition of $U = U_1 + U_2 + U_3$ implies that $\rho_F = \rho_{F1} + \rho_{F2} + \rho_{F3}$, $V_i = V_{i1} + V_{i2} + V_{i3}$ $(i = x, y, z)$, $p = p_1 + p_2 + p_3$, $e = e_1 + e_2 + e_3$ and $F_V = F_{V1} + F_{V2} + F_{V3}$, respectively. Thus the PML equations is thought as a generalize case of the non-viscous Euler equations, and those involve only the spatial derivatives of the total $\rho_F, V_x, V_y, V_z, p, e$ and F_V.
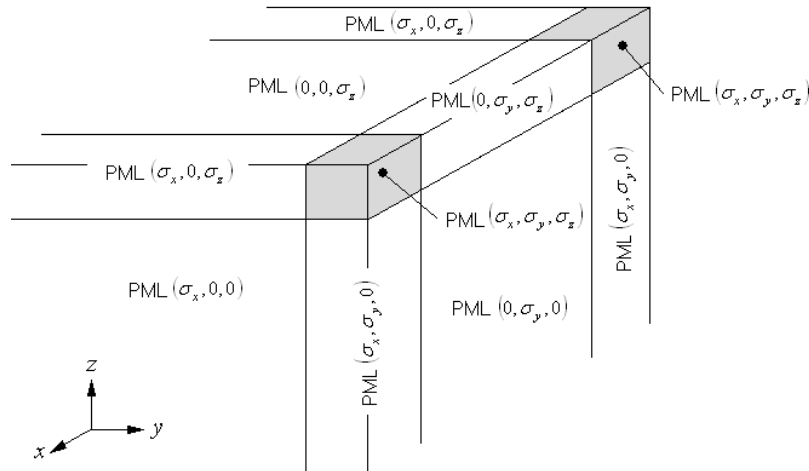

Fig. 2 A 3-D truncated simulation domain surrounded by the PML regions

4. NUMERICAL EXPERIMENTS

A 3-D coupled FVM-FEM model to simulate the platform-wave interaction induced by explosive is represented in Fig. 3, where the extended Euler domain is composed the lower water region and the upper void region. The depth of the simulation domain is set by $2m$, and the height and the diameters and the mean thickness of the platform are 1.332, $0.04 \sim 0.08$ and $0.0015m$, respectively. Three turbine blades, hub and nacelle are combined into a lumped mass, and three mooring cables are modeled using linear springs with the spring constant $k = 1.0 \times 10^6 \, N/m$. The rigid platform is modeled with 8-node hexahedron elements while the Euler region is discretized with 8-node cubic

elements. The total numbers of elements are 11,244 for the platform and 144,000 for the entire Euler region.
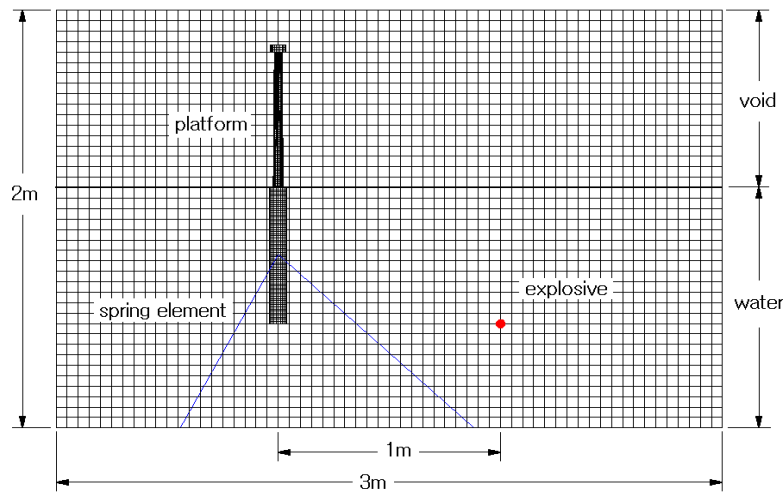

Fig. 3 A 3-D coupled FVM-FEM simulation model

A spherical LANL COMP B explosive with the radius of $0.112m$ and the internal energy $e_{INT} = 4.96 \times 10^6 J/kg$ is placed at the right side of the platform. The material properties are as follows: $\rho_F = 1,000 kg/m^3, K = 2.2 \times 10^9 N/m^2$ for water and the density of air is set by $1.225 kg/m^3$, respectively. The fluid-structure interaction simulation was carried out by MSC/Dytran (2006).
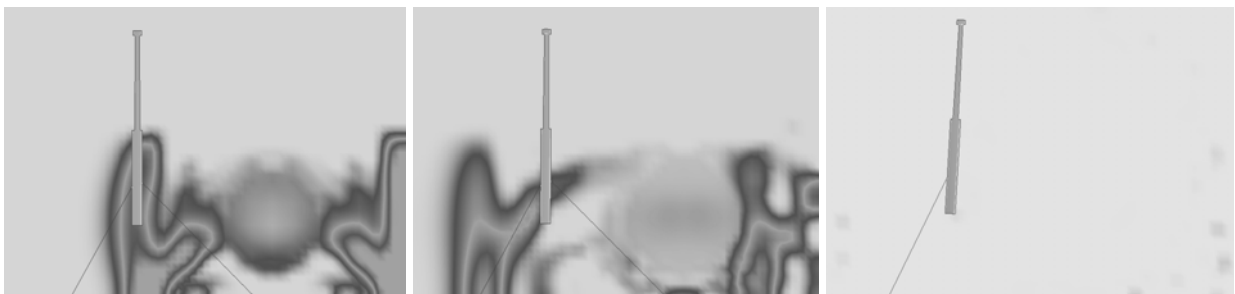

Fig. 4 Time histories of wave propagation without using the perfectly matched layer
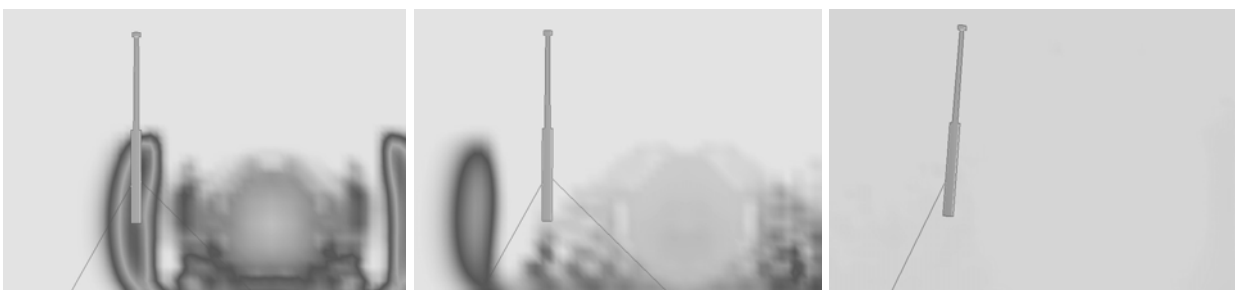

Fig. 5 Time histories of wave propagation using the perfectly matched layer

Fig. 4 shows the wave propagation and the platform motion at three different time

stages when the perfectly matched layer is not used. It is observed that the platform is significantly slanted at the final time stage and the explosive wave is reflected from the boundary. But, referring to Fig. 5, this remarkable wave reflection at the boundary is almost completely suppressed when the perfectly matched layer is employed.

CONCLUSION

A perfectly matched layer has been extended to the fluid-structure interaction of floating-type platform subject to under water explosion. The non-viscous compressible Euler equations are split into three sets by introducing the absorption coefficients. It has been confirmed from the numerical experiment that the use of perfectly matched layer successfully suppress the wave refection phenomenon at the boundaries of the truncated simulation domain.

ACKNOWLEDGEMENT

REFERENCES

Berenger, J-P. (1994) "A perfectly matched layer for the absorption of electromagnetic waves," *J. Comput. Phys.*, **114**(2), 185-200.

Cho, J..R., Lee, H.W., Sohn, J.S., Kim, G.J., Woo, J.S. (2006) "Numerical investigation of hydroplaning characteristics of three-dimensional patterned tire," *Eur. J. Mech. A/Solids*, **25**, 914-926.

Cho, J.R., Park, S.W., Kim, H.S., Rashed, S. (2008) "Hydroelastic analysis of insulation containment of LNG carrier by global-local approach," *Int. J. Numer. Methods Fluids*, **76**, 749-774.

Cho, J.R., Han, K.C., Hwang, S.W., Cho, C.S., Lim, O.K. "Mobile harbor: structural dynamic response of RORI crane to wave-induced excitation." *Struct. Eng. Mech.* (in press).

Hansen, A.D., Hansen, L.H. (2007) "Wind turbine concept market penetration over 10 years (1995-2004)." *Wind Energy*, **10**:81-97.

Hu, F.Q. (1996) "On absorbing boundary conditions for linearized Euler equations by a perfectly matched layer," *J. Comput. Phys.*, **129**, 201-219.

Karimirad, M., Meissonnier, Q., Gao, Z., Moan, T. (2011) "Hydroelastic code-to-code comparison for a tension leg spar-type wind turbine," *Marine Struct.,* **24**, 412-435, 2011.

Lee, E.L., Tarver, C.M. (1980) "Phenomenological model of shock initiation in heterogeneous explosive," *Phys. Fluids*, **23**(12), 2362-2372.

Lefebvre, S., Collu, M. (2012) "Preliminary design of a floating support structure for a 5MW offshore wind turbine," *Ocean Eng.*, **40**, 15-26.

MacNeal Schwendler Corp. (2006) *MSC/Dytran theory manual* (ver. 2005r3). Los Angeles, CA, USA.